Power Electronic Systems
Laboratory

Proceedings of the 14th IEEE Workshop on Control and Modeling for Power Electronics (COMPEL 2013), Salt Lake City, USA, June 23-26, 2013

Swiss Rectifier Output Voltage Control with Inner Loop Power Flow Programming (PFP)

P. Cortés,
F. Vancu,
J. W. Kolar

Eidgenössische Technische Hochschule Zürich
Swiss Federal Institute of Technology Zurich

Swiss Rectifier Output Voltage Control with Inner Loop Power Flow Programming (PFP)

P. Cortes, M. F. Vancu and J. W. Kolar
Power Electronic Systems Laboratory ETH Zurich
Physikstrasse 3, 8092 Zurich, Switzerland
Email: cortes@lem.ee.ethz.ch

***Abstract*—A novel control scheme is proposed for a three-phase buck-type SWISS rectifier. This control is based on an inner loop power flow programming that provides a well damped behavior of the output filter and decoupled input filter and converter dynamics. A DC/DC equivalent circuit of the SWISS rectifier is used for the analysis and evaluation of different control concepts for the switching stage of the converter. By using different feedforward loops for the calculation of the duty cycles the behavior of the converter can be modified to suit a desired characteristic. In this way, the converter can be programmed for constant voltage transfer ratio, constant output voltage, constant power transfer or other input/output relations.**

A comparative evaluation of different inner loop control schemes is presented. The control schemes are compared analytically using small-signal linear models. The comparison considers the dynamic behavior as well as the decoupling of the input and output variables. Simulation results using the DC/DC equivalent circuit model and the actual three-phase SWISS rectifier are presented. According to the results, the PFP control achieves an improved behavior of the converter in terms of damping of the resonances and decoupling of the input and output variables, compared to the other control schemes.

I. Introduction

Three-phase buck-type PFC rectifiers provide a wide range of output voltages, compared to a boost-type voltage source rectifier, while sinusoidal currents are maintained at the input. In addition, it is possible to limit the output current in case of a short circuit in the load. These characteristics make the buck-type rectifiers suitable for applications like electric vehicle battery chargers, power supplies or front-end for electric drives [1]–[3]. Among the different converter topologies that have been proposed in the literature, only the six-switch buck-type rectifier and the SWISS rectifier are of industrial interest [1].

Several control schemes has been proposed for three-phase buck-type rectifiers. Most of them consider the six-switch converter or a similar three-switch converter. The switching stage of the converter is modulated using hysteresis comparators [4], pulse-width modulation [5] or space vector modulation [6], while a cascaded control structure is usually considered for the output voltage control. An outer control loop regulates the output voltage and provides the reference for the inner control loop. There are two main options for the inner loop: control of the dc current [6] or control of the ac currents [4]. These two schemes have been compared and evaluated in [7]. A different approach uses the concepts of model predictive control (MPC) for a combined control and modulation of the rectifier for very low switching operation in [8] and for simultaneous control of the input and output in [9].

In this paper, different control concepts for a 5 kW SWISS rectifier shown in **Fig. 1** are evaluated. The control schemes are based on the analysis of the input/output relations in the power converter and the interaction between the converter and the input filter. A Power Flow Programming (PFP) control scheme is proposed for the inner loop. This control strategy provides a well damped behavior of the output filter and decoupled input filter and converter dynamics. An outer control loop is used for the output voltage. A DC/DC equivalent circuit of the SWISS rectifier is presented in **Section II**. This model allows a simpler evaluation and comparison of the control concepts explained in **Section III**. The dynamic behavior of the converter with the different schemes is analyzed in **Section IV**. Comparative simulation results are shown in **Section V**. The extension of the PFP concepts is discussed in **Section VI**. Conclusions are presented in **Section VII**.

II. Model of the SWISS rectifier

The SWISS rectifier is a PFC rectifier topology composed of a three-phase diode bridge with a third harmonic injection circuit, combined with a dc-dc buck converter (cf. **Fig. 1**). A detailed description and evaluation of this topology is presented in [2]. In this converter, the local average values of the currents in the switches T_p and T_n are modulated in order to be proportional to the phase voltages that define the output voltage of the diode bridge. The

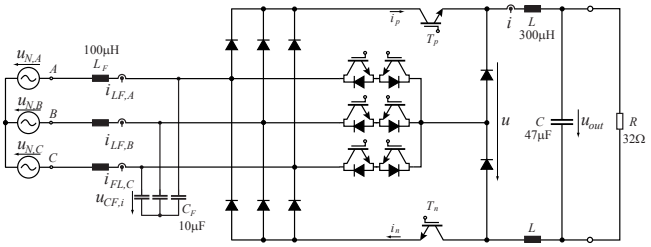

Fig. 1 Three-phase sinusoidal input current buck-type SWISS rectifier.

978-1-4673-4916-1/13/$31.00 ©2013 IEEE

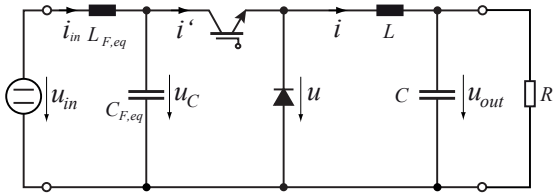

Fig. 2 DC/DC equivalent circuit of the SWISS rectifier.

bidirectional switches operate at twice the mains frequency and provide a path to feed the difference between the positive and negative currents, i_p and i_n, back to the phase voltage with lower absolute value. A 5 kW system with a switching frequency of 36 kHz is considered in this paper.

In order to simplify the analysis of the system dynamics and design of the different control concepts, a DC/DC equivalent circuit of the SWISS rectifier can be obtained, adapting to the buck topology the transformation principle proposed in [10] for a boost rectifier. In this equivalent circuit, the SWISS rectifier is modelled as a buck converter (cf. **Fig. 2**), and the input filter parameters are scaled to match the dynamics of the three-phase system ($L_{F,eq} = \frac{3}{2}L_F$, $C_{F,eq} = \frac{2}{3}C_F$ and $u_{in} = \frac{3}{2}\hat{u}_N$).

The relation between the averaged values of the input and output voltages and currents is defined by the duty cycle d of the switching device,

$$\bar{u} = d \cdot \bar{u}_C \tag{1}$$

$$\bar{i}' = d \cdot \bar{i}. \tag{2}$$

By using different relations and feedforward loops in the calculation of the duty cycle d, the input/output relations in the power converter can be modified to fit a specific requirement or a desired behavior. This idea has been used in [11] for providing a resistive behavior at the converter input. In addition to the resistive behavior, several other options are possible such as constant current, constant voltage or constant power transfer [12], which can be programmed for the input or for the output of the switching stage of the converter.

In this paper, different feedforward options are studied for application to the SWISS rectifier: constant input current, constant output voltage, constant power transfer and constant input resistance.

III. Control schemes

The control scheme for the SWISS rectifier considers an outer control loop for the output voltage u_{out} and an inner loop with different feedforward options. As a reference, the constant voltage transfer ratio scheme with no feedforward loops is also presented.

A. Constant voltage transfer ratio

A simple scheme way to calculate the duty cycle consists of scaling the reference voltage u^* by a constant value, the nominal input voltage u_{in}, i.e. $d = \frac{u^*}{u_{in}}$, as shown in **Fig. 3(a)**. In this way, a constant ratio between the converter output voltage u and the input filter capacitor voltage u_C, and between the input and output currents, i' and i, is established. These relations lead to interaction between the input and output filters, as it is depicted in the linearized model shown in **Fig. 3(b)**.

B. Constant input current

A method to decouple the input current from variations of the output current is implemented by including a feedforward loop of the output current i, as shown in **Fig. 4(a)**. By calculating the duty cycle using the actual value of the output current, $d = \frac{i'^*}{\bar{i}}$, the resulting input current is equal to its reference, $\bar{i}' = i'^*$. As shown in **Fig. 4(b)**, the linearized model presents no influence of the output filter dynamics in the behavior of the input current. However, there is a coupling from the input voltage to the output filter, and the feedforward loop introduces a negative feedback in the output filter dynamics that improves the damping of the output filter resonance.

C. Constant output voltage

A method to decouple the output voltage from variations of the input voltage is implemented by including a feedforward loop of the input capacitor voltage u_C, as shown in **Fig. 5(a)**. By calculating the duty cycle using the actual value of the input voltage, $d = \frac{u^*}{\bar{u}_C}$, the resulting output voltage is equal to its reference, $\bar{u} = u^*$. As shown in **Fig. 5(b)**, the linearized model presents no influence of the input filter dynamics in the behavior of the output filter. However, there is a coupling from the output filter to the input filter. In addition, the stability of the input filter is affected by the introduction of a positive feedback that needs to be compensated by the inclusion of a passive damping of the input filter.

D. Constant power flow programming

This control method is based on the power balance between the input and output of the switching stage of the converter, and denominated as Power Flow Programming (PFP) control. Given an output power reference P^*, provided by the output voltage controller, the required input current reference is calculated as

$$i'^* = \frac{P^*}{\bar{u}_C}, \tag{3}$$

then, by using the relation of input and output currents given by (2), the required duty cycle is expressed as

$$d = \frac{i'^*}{\bar{i}} = \frac{P^*}{\bar{i} \cdot \bar{u}_C}. \tag{4}$$

This method results in the inclusion of feedforward loops of the input capacitor voltage $\bar{u}_C$ and the output inductor current $\bar{i}$ [12], as shown in **Fig. 6(a)**. The PFP control provides a decoupled operation of the input filter and the output filter, which is reflected in the linearized model of the system shown in **Fig. 6(b)**. As observed in the model, a

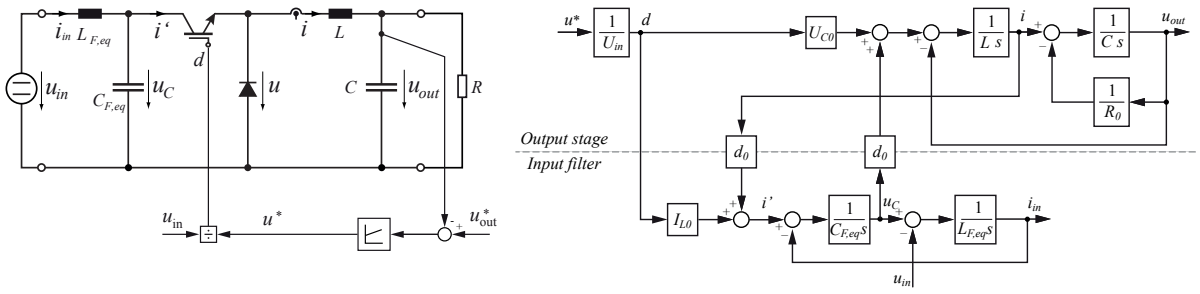

(a) DC/DC equivalent circuit and control (b) Linearized model (without the PI output voltage controller)

Fig. 3 Equivalent circuit of the SWISS rectifier with a constant voltage transfer ratio control scheme.

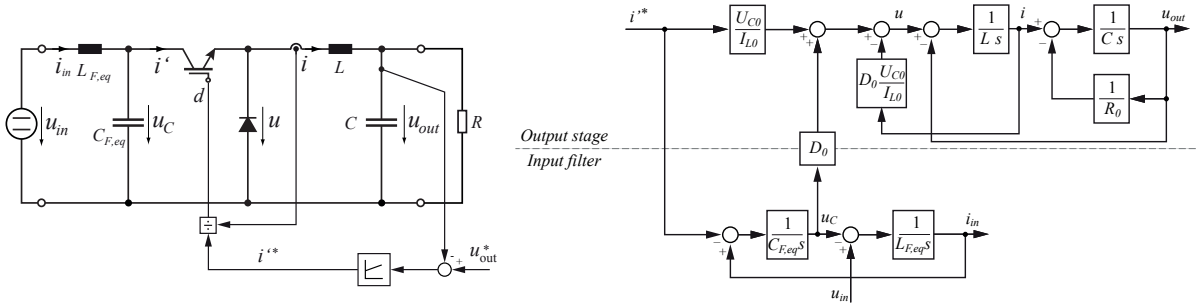

(a) DC/DC equivalent circuit and control (b) Linearized model (without the PI output voltage controller)

Fig. 4 Equivalent circuit of the SWISS rectifier with a constant input current control scheme.

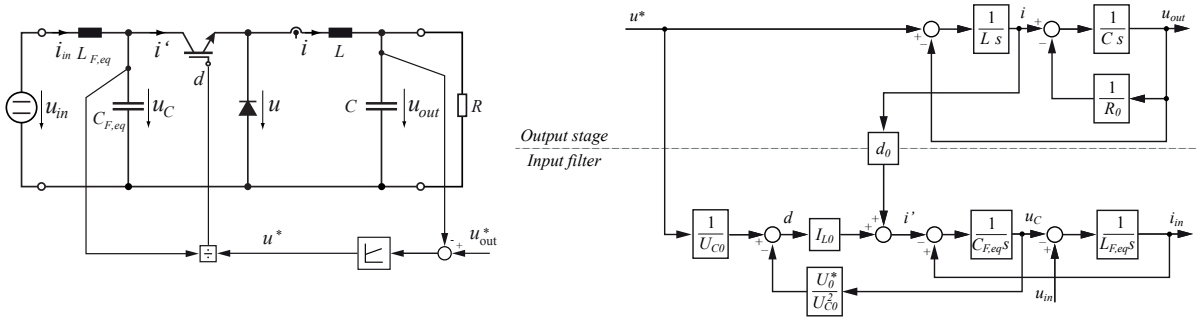

(a) DC/DC equivalent circuit and control (b) Linearized model (without the PI output voltage controller)

Fig. 5 Equivalent circuit of the SWISS rectifier with a constant output voltage control scheme.

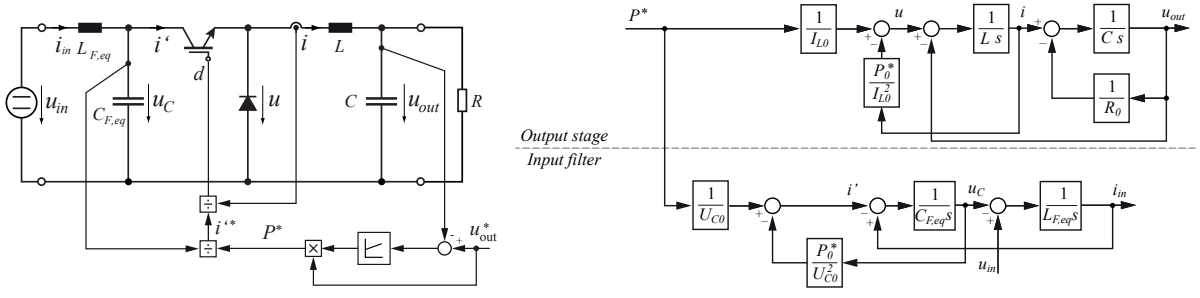

(a) DC/DC equivalent circuit and control (b) Linearized model (without the PI output voltage controller)

Fig. 6 Equivalent circuit of the SWISS rectifier with a constant interface power flow control scheme.

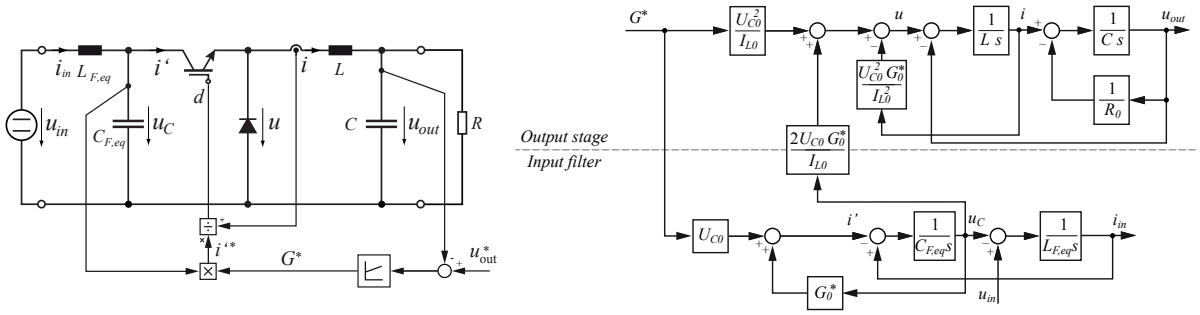

(a) DC/DC equivalent circuit and control

(b) Linearized model (without the PI output voltage controller)

Fig. 7 Equivalent circuit of the SWISS rectifier with a constant interface resistance control scheme.

positive feedback in the input filter is introduced, as in the case of the previous scheme. Regarding the output stage, a negative feedback of the inductor current is introduced, providing a damping of the output filter that improves the dynamic behavior of the output voltage.

E. Constant input resistance

In order to provide a resistive behavior at the input of the switching stage of the power converter, the ideas presented in [11] can be applied. Given a reference conductance $G^* = 1/R^*$, the required input current reference can be calculated as

$$i'^* = G^* \cdot \bar{u}_C, \tag{5}$$

and the required duty cycle is expressed as

$$d = \frac{i'^*}{\bar{i}} = \frac{G^* \cdot \bar{u}_C}{\bar{i}}. \tag{6}$$

The resulting control scheme is shown in **Fig. 7(a)**. This scheme introduces negative feedback in the input and output filter, improving the damping in both converter sides. However, there is coupling from the input to the output filter, as shown in the linearized model in **Fig. 7(b)**.

A summary of the input/output relations for the switching stage of the buck-type converter for the different feedforward control schemes is shown in **Table I**. These relations can be also depicted as a current/voltage curve for each control scheme, as shown in **Fig. 8**. The constant input current behavior is shown in **Fig. 8(a)** where the input current is independent of the voltage. A constant output voltage characteristic is shown in **Fig. 8(b)**. For a constant power transfer scheme, the input and output sides are operating at different points of the same constant power curve, as shown in **Fig. 8(c)**. A linear current/voltage relation is imposed with the constant input resistance scheme, as shown in **Fig. 8(d)**.

IV. Dynamic Behavior of the Control Schemes

Considering the linearized small-signal models of each control scheme, an equivalent circuit of the switching stage of the converter can be derived. As shown in **Fig. 9(a)**, the

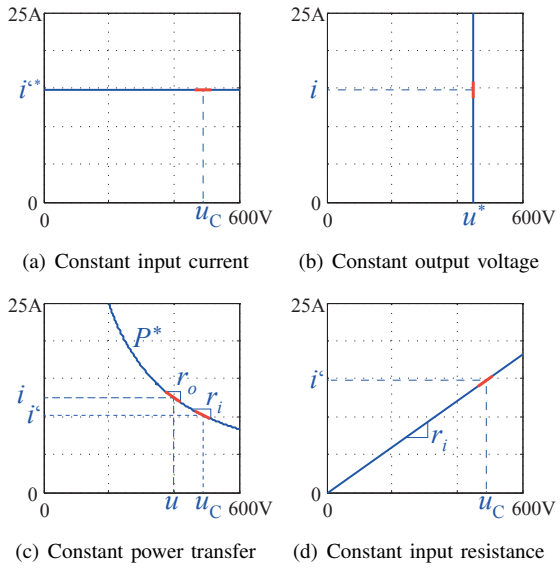

(a) Constant input current

(b) Constant output voltage

(c) Constant power transfer

(d) Constant input resistance

Fig. 8 Current/voltage relations in the switching stage of the converter for the different control schemes.

small-signal equivalent circuit for the constant input current scheme presents an ideal current sink at the input and an ideal voltage source with a positive inner resistance r_o at the output. The inner resistance r_o provides damping for the output filter resonance.

The equivalent circuit for the constant output voltage is shown in **Fig. 9(b)**, where the input side behaves as an ideal current sink with a negative parallel inner resistance r_i and the output side as an ideal voltage source.

The negative inner resistance is also present in the input side when the constant power transfer scheme is used, as shown in **Fig. 9(c)**. With this scheme, the output side presents a positive series inner resistance r_o.

In a constant input resistance scheme, positive inner resistances are present at the input and output sides, as shown in **Fig. 9(d)**, providing damping for the input and output filter.

TABLE I Input/output voltage and current relations for different control schemes.

Control scheme	*Voltage*	*Current*
Constant voltage ratio	$\bar{u} = \frac{u^*}{u_{in}} \bar{u}_C$	$\bar{i}' = \frac{u^*}{u_{in}} \bar{i}$
Constant input current	$\bar{u} = \frac{i'^* \bar{u}_C}{\bar{i}}$	$\bar{i}' = i'^*$
Constant output voltage	$\bar{u} = u^*$	$\bar{i}' = u^* \frac{\bar{i}}{\bar{u}_C}$
Constant power transfer	$\bar{u} = \frac{P^*}{\bar{i}}$	$\bar{i}' = \frac{P^*}{\bar{u}_C}$
Constant input resistance	$\bar{u} = \frac{G^* \bar{u}_C^2}{\bar{i}}$	$\bar{i}' = G^* \bar{u}_C$

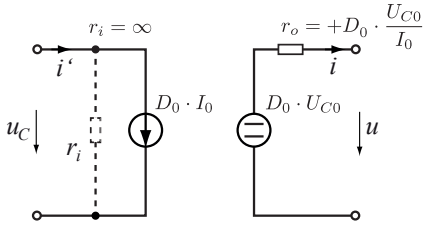

(a) Constant input current

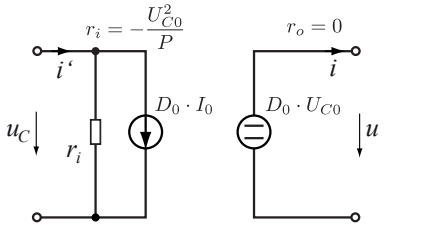

(b) Constant output voltage

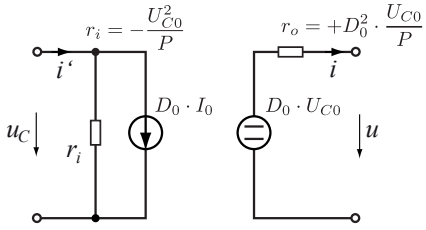

(c) Constant power transfer

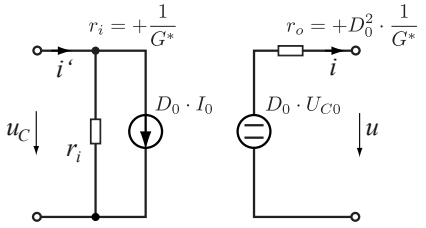

(d) Constant input resistance

Fig. 9 Small-signal equivalent circuit of the switching stage for the different control schemes.

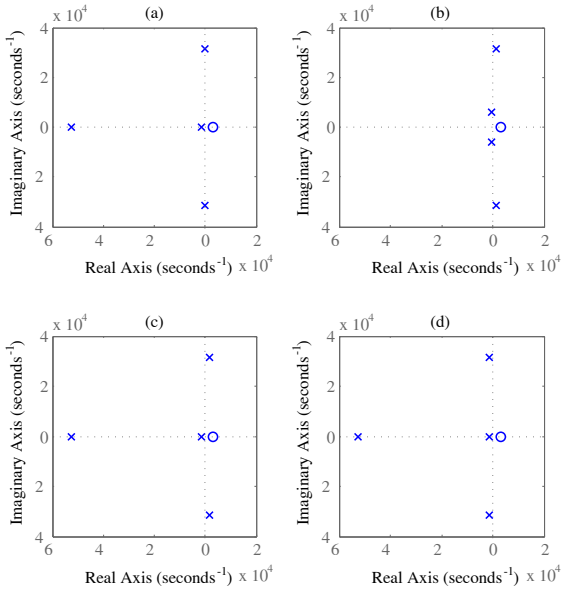

Fig. 10 Poles and zeros of the converter for the different control schemes.

The effect of the different control schemes in the placement of the converter poles and zeros is shown in **Fig. 10**. For a constant input current control, the output filter poles are located in the real axis, as shown in **Fig. 10(a)**, due to the damping provided by the inner resistance r_o, while the poles of the input filter remain undamped. In a constant output voltage scheme, the poles of the output filter are not damped and the poles of the input filter move to the right half-plane due to the negative inner resistance r_i at the input side, as shown in **Fig. 10(b)**. A similar behavior of the input filter poles can be observed when a constant power transfer scheme is used. However, the output filter poles are located in the real axis, as shown in **Fig. 10(c)**. For a constant input resistance scheme, both equivalent inner resistances, r_i and r_o are positive and the poles of the input and output filter are located in the left half-plane, as shown in **Fig. 10(d)**.

V. Results

Simulation results for the DC/DC model with the different control schemes are performed for open loop operation, i.e. the output voltage controller is omitted. A step change from 400 V to 450 V is applied in the value of the reference for the converter output voltage u^*. Results for the constant voltage ratio scheme [cf. **Fig. 5(a)**] are shown in **Fig. 11(a)**. The oscillations in the output voltage, due to the output filter resonance, are damped only by the load,

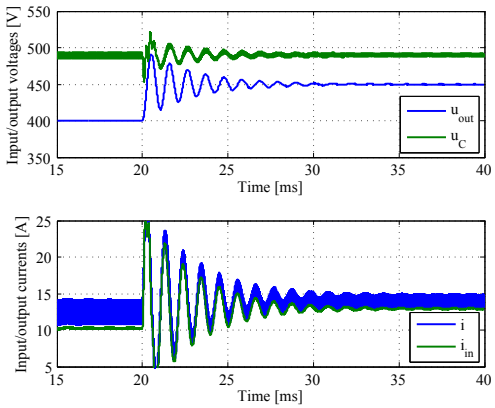

(a) Results using the equivalent DC/DC circuit.

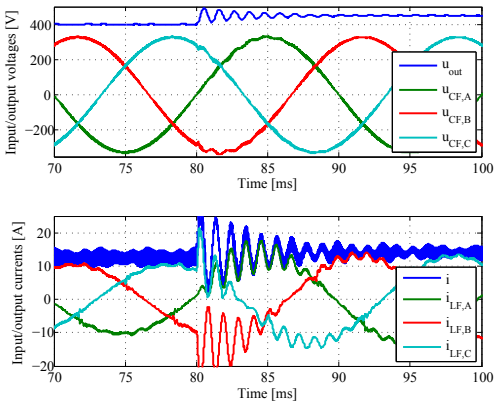

(b) Results for the three-phase buck-type SWISS rectifier.

Fig. 11 Simulation results for the constant output voltage control scheme (PFP, cf. **Fig. 5**). A step change in the converter output reference u^* is applied. The output voltage controller is omitted for these results.

and the oscillations in the output current are transferred to the input currents due to the coupling of the input and output dynamics. The same behavior is observed when the constant output voltage scheme is implemented for the SWISS rectifier, as shown in **Fig. 11(b)**.

Results using the constant power transfer control scheme [PFP, cf. **Fig. 6(a)**] for a step change in the reference power P^* for two different operating points are shown in **Fig. 12(a)** and **Fig. 12(b)**. A well damped response of the output voltage is observed and the oscillations of the input voltage are not transferred to the output voltage, demonstrating the decoupled operation of the converter. In order to verify the proposed control scheme, the constant power transfer control strategy is implemented for the SWISS rectifier. Simulation result for a step change in the reference power P^* is shown in **Fig. 12(c)**.The output voltage presents a well damped behavior and a decoupled response of the input filter is observed. A good match in the

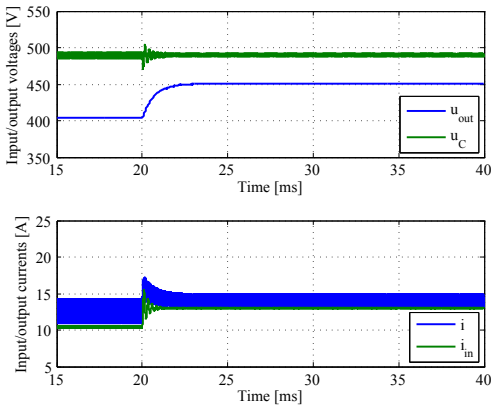

(a) Results for nominal power (equivalent circuit)

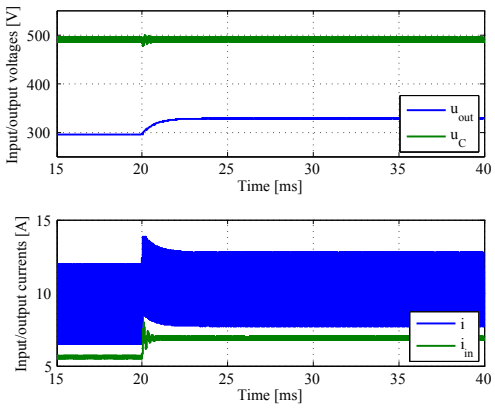

(b) Results for half nominal power (equivalent circuit)

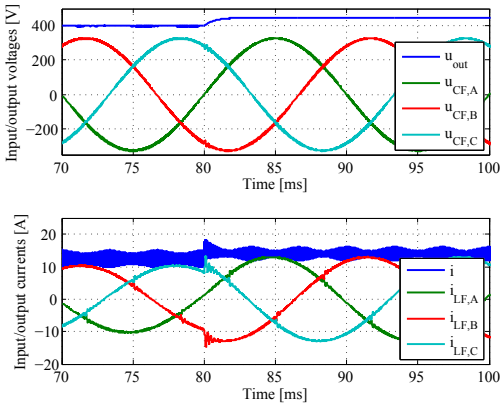

(c) Simulation result for the SWISS rectifier at nominal power

Fig. 12 Simulation results using the constant power transfer control scheme (cf. **Fig. 6**). The output voltage PI controller is omitted.

dynamic behavior of the three-phase system with respect to the DC/DC model is observed.

In order to evaluate the decoupling of the input and output filter dynamics, simulation results for a step change

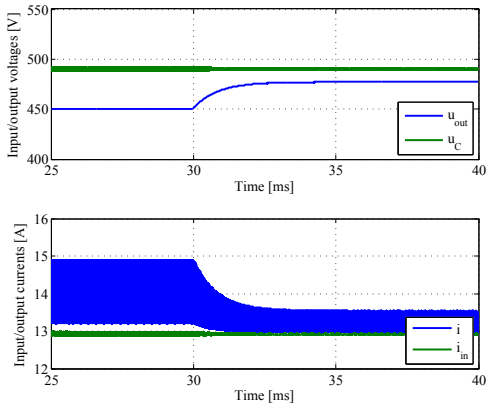

(a) Results for a step change in the load resistance from 32 Ω to 36 Ω.

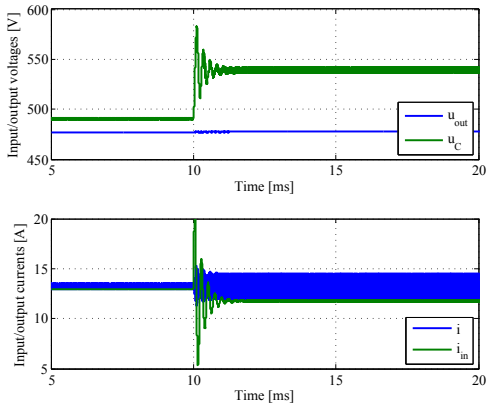

(b) Results for a 10 % step change in the supply voltage u_{in}.

Fig. 13 Simulation results for the constant power transfer control scheme (cf. **Fig. 6**). Evaluation of the decoupling between the input and output filter dynamics. The output voltage controller is omitted for these results.

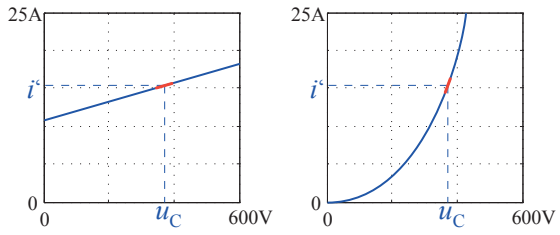

(a) (b)

Fig. 14 Nonlinear current/voltage relations in the switching stage of the converter.

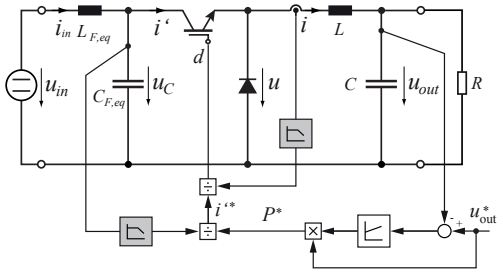

(a) Frequency shaping of the power transfer relations.

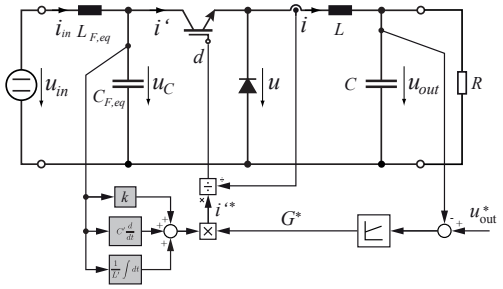

(b) Input impedance programming.

Fig. 15 Dynamic coupling in the switching stage of the converter.

in the load resistance are shown in **Fig. 13(a)** for a constant power transfer control scheme. As the reference power P^* is kept constant, the output voltage u_{out} increases and the output inductor current i decreases when the load resistance is increased. There is no noticeable effect of the load step in the input current and voltage. For a step change in the supply voltage u_{in}, the capacitor voltage u_C and the input current i_{in} change and strong oscillations are present during the transient, as shown in **Fig. 13(b)**. The output voltage u_{out} and current i are present no noticeable change, demonstrating the good decoupling achieved with the constant power transfer scheme.

VI. Further Extensions of PFP

A. Different programmed behaviors

In addition to the previously presented control schemes, the PFP schemes can be extended in several ways. The current/voltage relations in the switching stage can de defined as nonlinear relations, as shown in **Fig. 14**.

Furthermore, the couplings in the switching stage can be defined also in the frequency domain by introducing filtering in the feedforward loops, as shown in **Fig. 15(a)**. Another option considers the extension of the constant input resistance to a input impedance programming, by defining resistive, capacitive and inductive components in the calculation of the reference current i'^*, as shown in **Fig. 15(b)**.

B. Application to boost-type converters

The same concept of PFP control schemes can be applied to boost-type systems like the DC/DC converter shown in **Fig. 16**. By using feedforward loops of the input current i_{in} and/or the output voltage u_{out}, the following inner loop PFP schemes can be considered:

- Constant input voltage, where the duty cycle is calculated as $d = u^*/u_{out}$.

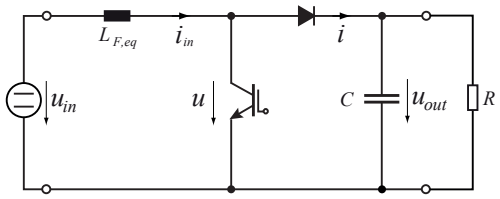

Fig. 16 Boost-type DC/DC converter.

- Constant output current, where the duty cycle is calculated as $d = i^*/i_{in}$.
- Constant power transfer, where the duty cycle is calculated as $d = P^*/(u_{out}i_{in})$.
- Constant output resistance, where the duty cycle is calculated as $d = G^*u_{out}/i_{in}$.

VII. Conclusions

This paper presents a new concept for the control of the buck-type SWISS rectifier. The control scheme considers an outer control loop for the output voltage and an inner feedforward loop for controlling the switching stage of the converter. Several feedforward options for the inner loop are analyzed and compared in terms of dynamics and coupling of the input and output sides. The proposed PFP control scheme with constant power transfer provides decoupling of the input and output filter dynamics and damping of the output filter resonance.

For the evaluation of the different control schemes a DC/DC equivalent circuit is used to model the SWISS rectifier dynamic behavior. This model allows a simpler analysis and assessment of the performance with the different schemes.

In addition to the basic schemes, the extension of the PFP concept is presented. The possible extensions include the use of nonlinear current/voltage relations, frequency shaping of the power transfer relations and the possibility of programming any type of impedance at the input of the switching stage of the converter.

The proposed control scheme is suitable for three-phase buck-type AC/DC converters and DC/DC converters, but it can be easily extended to other configurations such as boost-type rectifiers, inverters, and AC/DC/AC converters with and without energy storage.

References

[1] J. Kolar and T. Friedli, "The essence of three-phase PFC rectifier systems - Part I," *IEEE Transactions on Power Electronics*, vol. 28, no. 1, pp. 176–198, 2013.

[2] T. Soeiro, T. Friedli, and J. Kolar, "Swiss rectifier - A novel three-phase buck-type PFC topology for electric vehicle battery charging," in *Proceedings of the 27th Annual IEEE Applied Power Electronics Conference and Exposition (APEC)*, 2012, pp. 2617–2624.

[3] T. Nussbaumer, G. Gong, M. Heldwein, and J. Kolar, "Control-oriented modeling and robust control of a three-phase buck+boost PWM rectifier (VRX-4)," in *Proceedings of the 40th IEEE Industry Applications Society Annual Meeting*, vol. 1, 2005, pp. 169–176.

[4] N. Zargari and G. Joos, "A current-controlled current source type unity power factor PWM rectifier," in *IEEE Industry Applications Society Annual Meeting*, vol. 2, Oct. 1993, pp. 793 – 799.

[5] T. Nussbaumer and J. Kolar, "Advanced modulation scheme for three-phase three-switch buck-type PWM rectifier preventing mains current distortion originating from sliding input filter capacitor voltage intersections," in *Proceedings of the IEEE 34th Annual Power Electronics Specialist Conference (PESC '03)*, vol. 3, June 2003, pp. 1086 – 1091.

[6] G. Marques, "A PWM rectifier control system with DC current control based on the space vector modulation and AC stabilisation," in *Proceedings of the 7th International Conference on Power Electronics and Variable Speed Drives (Conf. Publ. No. 456)*, Sept. 1998, pp. 74 – 79.

[7] T. Nussbaumer and J. Kolar, "Comparative evaluation of control techniques for a three-phase three-switch buck-type AC-to-DC PWM converter system," in *Proceedings of the Nordic Workshop on Power and Industrial Electronics (NORPIE '02)*, Aug. 2002.

[8] P. Correa, J. Rodriguez, I. Lizama, and D. Andler, "A predictive control scheme for current-source rectifiers," *IEEE Transactions on Industrial Electronics*, vol. 56, no. 5, pp. 1813 – 1815, May 2009.

[9] P. Cortes, J. Kolar, and J. Rodriguez, "Comparative evaluation of predictive control schemes for three-phase buck-type PFC rectifiers," in *Proceedings of the 7th International Power Electronics and Motion Control Conference (IPEMC)*, vol. 1, 2012, pp. 666–672.

[10] H. Mao, D. Boroyevich, and F. Lee, "Novel reduced-order small-signal model of a three-phase PWM rectifier and its application in control design and system analysis," *IEEE Transactions on Power Electronics*, vol. 13, no. 3, pp. 511–521, 1998.

[11] S. Singer, "Realization of loss-free resistive elements," *IEEE Transactions on Circuits and Systems*, vol. 37, no. 1, pp. 54–60, 1990.

[12] R. King, "Feedforward control laws for the buck converter," in *Proceedings of the IEEE 4th Workshop on Computers in Power Electronics*, 1994, pp. 192–197.